Renewable Energy 143 (2019) 164–175

Contents lists available at ScienceDirect

Renewable Energy

journal homepage: www.elsevier.com/locate/renene

Capacity credits of wind and solar generation: The Spanish case

Pablo Tapetado*, Julio Usaola

Department of Electrical Engineering, Universidad Carlos III de Madrid, Leganés, Madrid, Spain

ARTICLE INFO

Article history:
Received 21 July 2018
Received in revised form
20 March 2019
Accepted 25 April 2019
Available online 2 May 2019

Keywords:
Capacity credit
Power system reliability
Capacity value
Equivalent firm capacity
Sequential Monte Carlo simulation
Loss of load expectation

ABSTRACT

This paper analyses the capacity credits (CCs) of renewable photovoltaic (PV), concentrated solar power (CSP) and wind technologies in the Spanish power system. This system has steadily increased the share of renewables, reaching a penetration level of over 30%. The predictions made by ENTSO-e suggest that this level will increase to 50% by 2030. Therefore, different scenarios are studied in this paper to investigate the evolution of renewable integration and assess the corresponding contributions to reliability. The assessment is performed using a sequential Monte Carlo (SMC) method considering the seasonality of renewable generation and the uncertainties related to renewable sources, failure issues and the maintenance of thermal-based units. The baseline for SMC is provided by historical annual time series of irradiance and wind power data from the Spanish system. In the solar case, these time series are transformed into power time series with models of CSP and PV generation. The former includes different thermal storage strategies. For wind generation, a moving block bootstrap (MBB) technique is used to generate new wind power time series. The CC is assessed based on the equivalent firm capacity (EFC) using standard reliability metrics, namely, the loss of load expectation (LOLE). The results highlight the low contribution of renewables to power system adequacy when the Spanish power system has a high share of renewable generation. In addition, the results are compared with those of similar studies.

1. Introduction

Each year, electrical power systems integrate a greater amount of renewable power. Many of the countries that have embraced this trend use renewable energy to meet the climate objectives issued by the respective administrations. Additionally, countries used renewable sources as a way to reduce their expenses, produce energy and increase their efficiency. In 2017, the Spanish power system had a total installed capacity of 99.31 GW, of which 30.5% was associated with renewable generation, mostly from wind and solar [1].

However, only 25.5% of the energy was supplied by these renewable sources. The European Energy Commission predicts that the installed renewable capacity, without considering hydropower, will reach 50% by 2030. This commission foresees installed power capacities of 34.5 GW, 25.8 GW and 6.1 GW for wind, photovoltaic (PV) and concentrated solar power (CSP), respectively. These levels require increases of 11.7 GW of wind power, 21.4 GW of PV power and 3.8 GW of CSP compared to the currently installed capacities. The remarkable increase in photovoltaic technology is mainly due to the reduction in the corresponding operating and capital costs. Therefore, it is necessary to assess the contribution of PV power to the adequacy, which is related to reliability, of the Spanish power system. This work focuses on the most widely used renewable energy sources in Spain: wind and solar. Wind technology is advanced in Spain due to the high installed power capacity and future potential. Likewise, the Iberian Peninsula is a suitable location for solar exploitation. In particular, CSP technology has been used over the past 10 years in Spain due to the feasibility of this technology in sunny regions, the high dispatch capacity and storage capability, and advances in both gas and biomass hybridization techniques.

Power system planners and operators aim to provide reliable and cost-effective electricity to their customers. The desired level of reliability is normally achieved using spare or redundant generation capacity and network facilities to compensate for the generation shortage (unexpected or planned) or the lack of available generation from renewable sources. To eliminate or reduce excessive redundancy, appropriate reliability assessments are required in the planning (long term and mid-term) and operational phases (short term). Reliability evaluations in both phases can be

* Corresponding author.
E-mail addresses: ptapetad@ing.uc3m.es (P. Tapetado), jusaola@ing.uc3m.es (J. Usaola).

https://doi.org/10.1016/j.renene.2019.04.139
0960-1481/

Abbreviations

ARIMA	Autoregressive Integrated Moving Average
CC	Capacity Credit
CSP	Concentrated Solar Power
CV	Capacity Value
ECPP	Equivalent Conventional Power[1] Plant
EFC	Equivalent Firm Capacity
ELCC	Equivalent Load Carrying Capability
ENTSO-E	European Network of Transmission System Operators
GADS	Generating Availability Data System
LOEE	Loss of Energy Expectation
LOLE	Loss of Load Expectation
MAF	Mid-term Adequacy Forecast
MBB	Moving Block Bootstrap
NERC	North American Electric Reliability Corporation
NG	New Generation
NREL	National Renewable Energy Laboratory
PC	Perfect Capacity
PSB	Power System Base
PV	Photovoltaic
SAM	System Advisor Model
SMC	Sequential Monte Carlo
WWSIS	Western Wind and Solar Integration Study

conducted with methods that are divided into two groups: deterministic and probabilistic methods. Both methods are presented in Fig. 1 and explained in Refs. [2,3]. Deterministic methods have been developed from the experience of system planners and are commonly used due to their simplicity. For instance, typical approaches have focused on the percentage of the reserve margin needed or the failure of the largest generation unit in the system [4]. Probabilistic methods consider the stochastic behaviour of thermal-based[2] generation availability and renewable generation uncertainty; therefore, they have been chosen to evaluate reliability in this work. It must be stressed that probabilistic methods yield higher accuracy than deterministic methods because they consider a wider range of scenarios (wind, solar, the demand, available generation, etc.)

To date, few mid-term and long-term adequacy studies have considered the inclusion of renewable supplies. International commissions such as the North American electric reliability corporation (NERC) [5], national renewable energy laboratory (NREL) [6,7] and European network of transmission system operators (ENTSO-E) [8] have performed reliability studies of adequacy and security. Adequacy is defined as the existence of sufficient facilities in a system to satisfy the consumer demand [2], and security is defined as the ability of the system to respond to a disturbance that arises within the system. The methodologies most commonly used to assess these reliability characteristics have been published in Refs. [8–10] by the NERC and ENTSO-E. Within these organizations, only the NERC clearly defines the capacity credit (CC) as follows: "*how much a particular generator or group of generators contribute towards planning reserve, given a reliability target*". The NREL and ENTSO-E do not give a specific CC definition.

The contribution to the reliability, or specifically, the adequacy, of a power system from a single supply source is measured through CC or capacity value (CV) evaluations. The current CC definitions widely vary, and examples are given in Refs. [11–13]. The definitions that are commonly used are as follows.

- Equivalent load carrying capability (ELCC) is defined as the possible load increase when a generator is added while maintaining the reliability of the system.
- Equivalent firm capacity (EFC) is defined as the capacity of a fully reliable generator or an ideal power plant that can replace the added generator while maintaining the reliability of the system.

[1] Conventional power unit: a power unit in which the energy is obtained by a combustion of coal, hydrocarbons or by a nuclear reaction.

[2] Thermal-based power units: a power unit in which electricity is generated by conversion of thermal energy (CSP units are included).

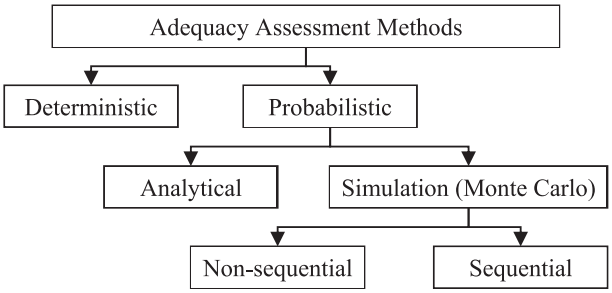

Fig. 1. Classification of reliability assessment methods.

- Equivalent conventional power plant (ECPP) is the same as EFC but for a conventional power plant with a specific failure rate.

The accuracy assessments of these methods involve long calculation times and significant computational effort. Thus, some definitions based on approximations have been proposed. For instance, capacity factor-based methods (Top-load, Top-LOLP and LOLP weighted) were discussed by Madaeni et al. in Ref. [13]. These methods focus on periods of low reliability and compared power consumption and power generation for an added generator. Summaries of these parameters can be found in Refs. [6,7].

Regarding the CC evaluation results, some studies have analysed the contribution of CSP to the reliability level. The studies of Madaeni et al. [13,14] provided the CV of CSP plants with and without thermal storage in a case study in the southwestern United States. These studies used the approximation methods Top-load, Top-LOLP and LOLP weighted. Another study [15], assessed the CC of CSP plants using the Reliability Test System [16]. Another CC result for wind technology can be found in Ref. [11] and in a western wind and solar integration study (WWSIS) report [6]. In the case of PV CC results, WWSIS also included a CC analysis as did a recent study by Ding et al. [17].

The objectives and contributions of the paper are twofold. The first objective is to provide a baseline for assessing reliability evaluations in the Spanish power system. Notably, the modelling in this study combines different models of renewable technologies to represent the entire system. The second objective is to determine the effects and contributions to the reliability of renewable technologies in future scenarios involving the Spanish power system. To the knowledge of the authors, a thorough study of the CCs of renewable technologies with different methodologies in a multi-renewable generation scenario in a power system is not available in the literature. These studies are necessary for power system planning with a large share of renewables.

2. Methodology

This section explains the sequential Monte Carlo (SMC) simulation tool used in reliability evaluations based on a probabilistic approach and the algorithm used in the CC evaluation. The reliability analysis based on adequacy, the focus of this study, represents the ability of generation facilities to meet the total system load by assuming that energy is produced and consumed at a single node.

2.1. Reliability evaluation

The results provided by probabilistic methods are typically represented by reliability indices, such as loss of load expectation (LOLE) or loss of energy expectation (LOEE). The LOLE index is the average number of hours per year in which the demand is expected to be higher than the available capacity. In contrast, the LOEE index is the average energy expected to not be supplied by the available generation capacity.

The methodology used to calculate the reliability indices is given in Fig. 2. This methodology is based on Monte Carlo simulations. The procedure begins with the compilation of the generation capacity time series for thermal-based power units. All these units have probability distribution functions involving failure and repair, which are exponential. Likewise, renewable generation is associated with a certain variability in resource availability due to the uncertainty associated with each resource. For these reasons, the construction of the available generation time series should be based on random sampling and the associated distribution functions. Due to the large number of power units in the system, which involve many random variables, analytical methods must be discarded in favour of Monte Carlo simulations. In particular, the methodology used is the SMC. The SMC performs sequential random sampling and considers the history of the events, which is necessary to build correlated time series of renewable resources.

The algorithm presented in Fig. 2 obtains the LOLE value as the average of the number of lacking generation hours annually. This average converges to the final value after a number of iterations. The solution is found when the value of β in Eq. (1) is lower than a given tolerance.

$$\beta = \frac{\sqrt{\mathrm{var}(E[\mathrm{LOLE}])}}{E[\mathrm{LOLE}]} \tag{1}$$

where E is the expected value and *var* is the variance for all years evaluated. In addition, β and the maximum number of simulated years (y_{max}) are the stopping criteria of the reliability algorithm. The stopping rules are used to avoid long calculation times and to use as few sampling years as possible for each LOLE calculation.

2.2. Capacity credit evaluation and EFC methodology

The CC algorithm used, which is based on the EFC methodology, is presented in Fig. 3. The reliability indices of the two systems are compared to evaluate the CC. System 1 is composed of a power system base (PSB), which is the same as in system 2, and the aggregated new generation (NG) from the technology to be studied (CSP, Wind or PV). System 2 also adds the perfect capacity (PC) unit to the PSB based on which the CC is assessed. The PSB, in turn, is composed of the elements (load, conventional capacity and the remaining renewable capacity) that do not change for the two systems created (2).

After the two systems are defined, the algorithm modifies the capacity of the PC, which is a fully reliable unit, and the reliability level of system 2 is calculated. The objective is to determine how much new capacity is needed in system 2 to match the reliability level of system 1.

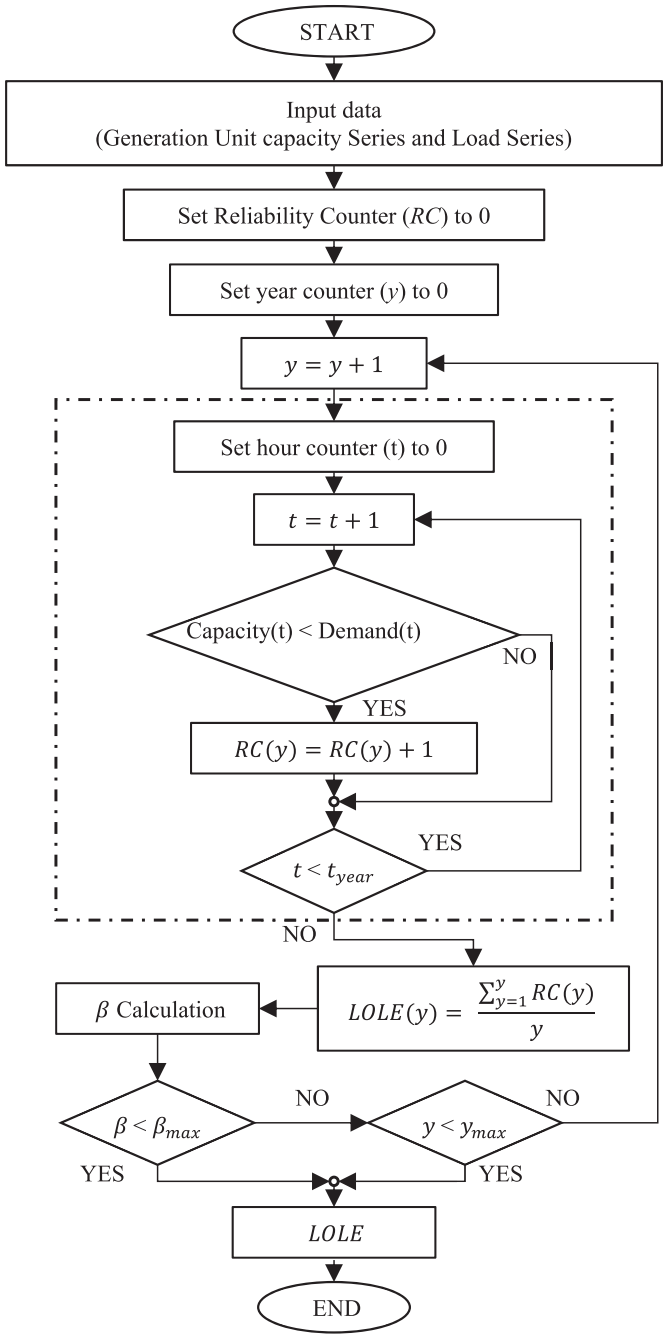

Fig. 2. SMC reliability evaluation algorithm.

$$\begin{aligned} &LOLE_{System\ 1} = LOLE_{System\ 2} \\ &\left.\begin{array}{l} System\ 1 \ \rightarrow \ G_{PSB} + G_{NG} = D \\ System\ 2 \ \rightarrow \ G_{PSB} + G_{PC} = D \end{array}\right\} \end{aligned} \tag{2}$$

In (2), G_{PC} is the equivalent capacity of the ideal power plant, G_{NG} is the new installed capacity and D is the demand. Therefore, the EFC, which is expressed per unit (p.u.), is defined as follows.

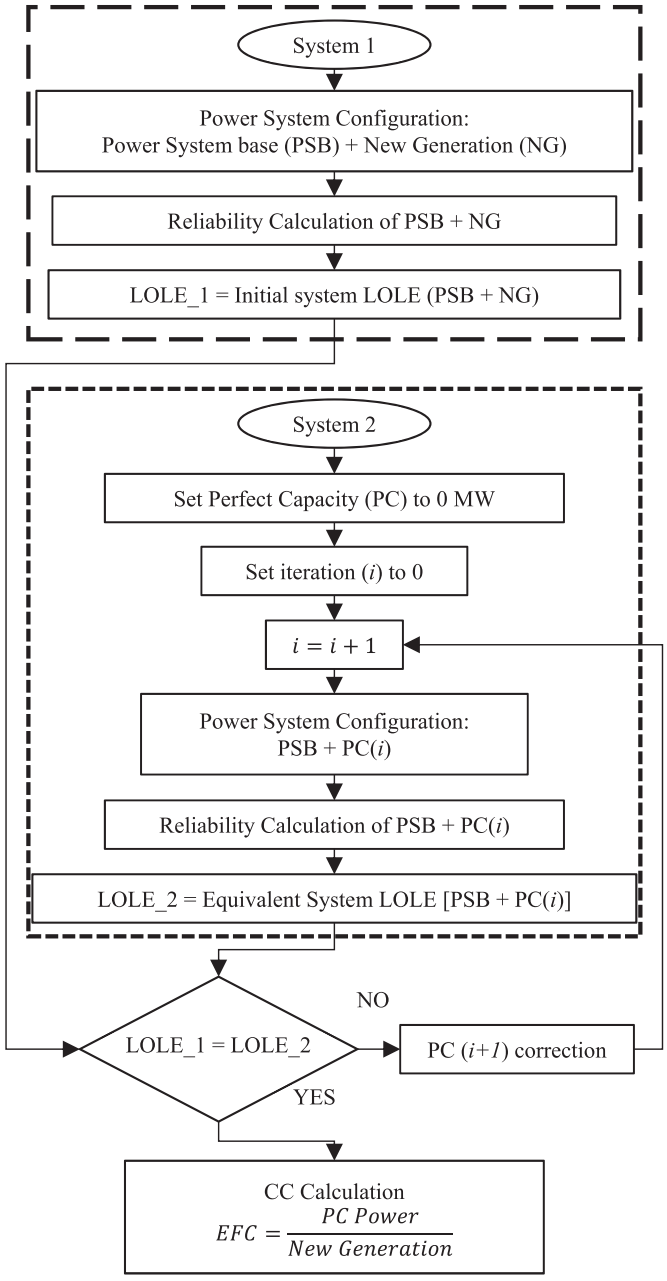

Fig. 3. CC algorithm.

$$EFC = \frac{G_{PC}}{G_{NG}}(p.u) \quad (3)$$

The EFC evaluation has been chosen for the following reasons.

- The EFC, as defined in section 1, compares the contribution of a power source with that of an ideal generator or fully reliable generator. This approach avoids the choice of new generator reliability.
- The NREL compares the contribution of a power source to that of a fully reliable generator applying another methodology to provide the results in Ref. [6]. The EFC favours a comparison between studies.
- From a computational perspective and according to Fig. 3, the EFC algorithm replaces the NG in system 2 with a PC. The model that represents the NG is not included in system 2. This approach reduces the complexity of system 2 and helps save computational time. In contrast, the ELCC algorithm must consider the NG in system 2.

3. CSP and PV model descriptions

The reliability evaluation and CC assessment presented in the previous section focus on future power systems. These analyses involve using a large amount of data to represent their behaviour. Hence, simplified PV and CSP models are needed to reduce the computational effort. Both the CSP and PV models are based on a combination of different submodels that represent the energy conversion from solar radiation to electricity generation. The submodels for each step are selected from the current state-of-the-art methods, although the main criterion for model selection is related to their suitability for SMC.

The PV generation model used is taken from Ref. [18]. In this study by Santos-Martin et al., a full explanation of solar device equations is given. This PV model is suitable for representing the intermittent behaviour of clouds, which affects PV power delivery.

In the case of the CSP model, the irradiance conversion equations from the PV model can be applied to the CSP model due to its similar nature, except that CSP plants only use the beam irradiance in thermal conversions. A schematic characterization of CSP plant conversion processes is provided in Fig. 4. Regarding thermal management, thermal storage and thermal to electricity conversion, Gafurov et al. [15] presented a novel CSP model in which the power output delivered to the net was compared with the results provided by the software system advisor model (SAM) [19]. The differences between the results of both models were also compared, and Gafurov's model was shown to be acceptable for use in long-term adequacy studies. It should be noted that the model uses a small number of input values without loss of accuracy.

For CSP units, this study uses the storage modelling method in Ref. [20] because storage characterization is used to model a real CSP plant in Spain and the formulation used is easy to implement, which provides a suitable storage model for SMC calculation. A detailed storage model can increase the calculation time of the iterative process in the evaluation of adequacy. Finally, the formulation facilitates the application of different strategies for the discharge of storage. Using different storage strategies is a novel

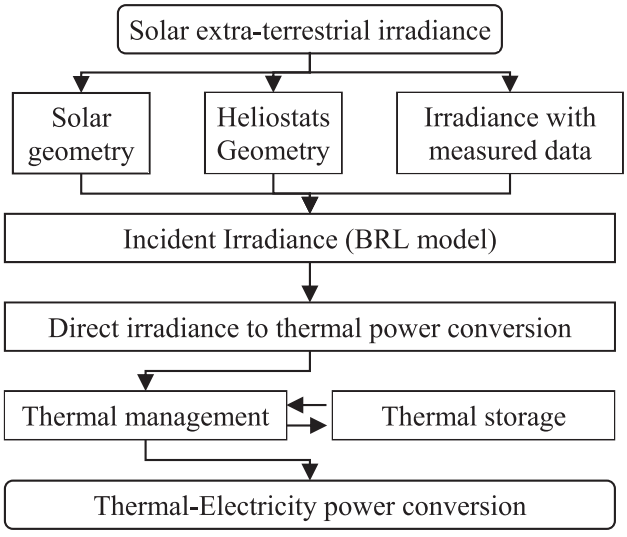

Fig. 4. Schematic characterization of the CSP model.

task that is developed in this work.

The CSP model is summarized in Table 1, in which the main equations of thermal power management and storage are shown. The nomenclature used is explained in Table 2. The thermal power generation in the solar field is represented in Eq. (4), and the power flows through the plant according to Eq. (5). Equation (6) defines the warming requirements. The storage management scheme with capacity, charging rate and discharging rate boundary conditions is established in Eq. (7) and Eq. (8). Finally, the gross power and net power output are represented by Eq. (9) and Eq. (10).

4. Wind power model

As discussed in the CSP and PV model description section, the solar intermittent behaviour is represented by the use of historical hourly irradiance data. Similarly, historical hourly wind speed data are used in the case of wind power and are available in Ref. [21]. The wind speed data were collected from weather stations located at different places. Despite the availability of existing wind data, the transformation from wind speed to farm power output is complex. First, the measured wind speeds must be transformed to obtain the actual input of wind farms because weather stations are not located at the wind farm sites. Second, a proper wind farm model is also needed to obtain the output wind power.

The solution to reducing the complexity is to use historical wind power time series from Spain. In the case of Spain, the available data in Ref. [22] are insufficient for use in reliability assessments, and the generation of synthetic power time series is needed. A possible solution is to use autoregressive integrated moving average (ARIMA) methods or other time series-based models. For instance, such methods are used in Ref. [23] to reproduce the production of a wind farm and in Ref. [24] to create the production time series for the UK.

Due to the complexity of applying the ARIMA method along with SMC, this study chooses the moving block bootstrap (MBB) method to generate synthetic hourly wind power time series from existing historical data for a wind production system. This method consists of the sequential construction of a wind power time series based on the random sampling of blocks from different historical wind power time series. This technique is used in Ref. [25] for the same purpose as in this study. The objective is to create sufficient power time series for the SMC simulation. However, this method can only be used when there is a significant quantity of time series data for wind production. Even in these cases, the method cannot consider possible future changes in production patterns. In the case of Spain, with a large installed capacity that is geographically distributed and with production records for several years, this approach is a valid choice.

Table 1
Equations for thermal CSP management.

Equation	Number
$E_t = K^{SM} G_t^{bi} A^{SF} \eta^{SF} \cos(\Theta_t)$	(4)
$E_t = j_t^{Warm} + j_t^{SF-E} + j_t^{SF-S} + j_t^{Loss}$	(5)
$E^{Warm} = \sum_{t \in W} j_t^{Warm}$	(6)
$J_t^S = J_{t-1}^S + j_t^{SF-S} - j_t^{S-E}$	(7)
$\begin{cases} J^{Min} \le J_t^S \le J^{Max} \\ J_{t-1}^S - J_t^S \le J^{Dw}/F^{dis} \\ J_t^S - J_{t-1}^S \le J^{Up} \end{cases}$	(8)
$p_t^{Gross} = \eta^T \eta_t^{Corr} (j_t^{SF-E} + \eta_s^S j_t^{S-E})$	(9)
$p_t^{Net} = p_t^{Gross} - p_t^{PL}$	(10)

5. Spanish power system

The reliability study was applied to the Spanish Peninsular power system. This power system includes wind, hydropower, PV, CSP and pumping hydro and conventional generators. The technologies not included in Table 3 are considered fully reliable.

5.1. Conventional thermal generation

The conventional thermal power generation capacity consists of 31 coal units (10.46 GW of installed capacity), 51 combined cycle units (24.94 GW of installed capacity) and 7 nuclear units (total of 7.11 GW of installed capacity). The total installed capacity is 42.53 GW. All the capacity and reliability characteristics of these units are summarized in Table 3, in which the units are grouped in power intervals based on the technology. The reliability characteristics of the generating units are collected from the NERC's generating availability data system (GADS) [26]. For wind and hydropower generation, power time series from 2014 to 2017 are considered. The power time series data were obtained from the Spanish TSO webpage [22].

5.2. Load

To represent the Spanish load, the annual load profiles from 2014 to 2017 are considered. The load profile data were collected from the Spanish TSO webpage [22]. The 4 years of collected data reflect changes in the load between years. In addition, by subtracting the correlated power time series from the wind power, hydropower and solar power data, a residual (net) load can be established. The net load is the corresponding load that thermal generation must supply. Both the original and net loads are shown in Fig. 5(a) where the first week of January in the four years is illustrated. Examples of the use of net load profiles to assess hydropower reliability can be found in Refs. [27,28]. These studies, which focused on the Spanish power system, employed net load data because the hydraulic component is important in the Spanish peninsula region.

5.3. CSP plants

Referring to the added CSP power plants, the design is based on parabolic trough CSP plant technology, which has been described in the model used. The design parameters were taken from SAM [19]. The main parameter of the plant is the rated power, which is 100 MW. At night, the power consumption of each plant is 1.51 MW. The storage is scaled to supply energy for 7 h at the rated capacity. The solar field has a solar multiplier of 2.5. The solar field, storage and steam turbine have efficiencies of 0.76, 0.95 and 0.37, respectively. The reliability characteristics of the CSP plants are summarized in Table 3. Finally, eight different locations where CSP plants can be placed in Spain because of the available resources are considered in the CC assessment to distribute the overall electricity output from CSP plants. The solar irradiation data used as inputs to the CSP model include 14 years of hourly irradiance at each location.

The modification to the CSP model that this work introduces is the discharge control. The objective of this control is to regulate the thermal storage and control the power output of the CSP. Thus, the CSP output can be adjusted to meet the demand requirements. This adaptation consists of an attempt to fit the power output of the CSP plant to the load consumption trend. A good correlation between the load and generation improves the reliability of the power system [29]. Three discharge strategies are proposed to consider extreme scenarios and assess the corresponding effect on

Table 2
CSP management nomenclature.

Greek symbols	
η^{Corr}	Efficiency correction of the steam turbine. (p.u.)
$\eta^{S/SF/T}$	Efficiency of storage/solar filed/steam turbine (p.u.)
Θ_t	Angle (degrees)
Roman symbols	
A^{SF}	Solar field area (m^2)
E_t	Solar field power production (W-t)
E^{Warm}	Total energy for warming up (Wh-t)
F^{Dis}	Maximum power delivered from storage alone (p.u.)
G_t^{bi}	Beam (direct) incident irradiance (Wm^{-2})
$J^{Min/Max}$	Min/Max thermal energy in the storage (Wh-t)
J_t^S	Thermal energy in the storage (Wh-t)
$j^{Dw/Up}$	Up/down thermal ramp rate in the storage (W-t)
j_t^{Loss}	Thermal power spillage (W-t)
j_t^{S-E}	Thermal power from storage to electricity (Wh-t)
j_t^{SF-E}	Thermal power from solar field to electricity (W-t)
j_t^{SF-S}	Thermal power from solar field to storage (W-t)
j_t^{Warm}	Thermal power from solar field to warm up (W-t)
K^{SM}	Solar multiple (p.u.)
p_t^{PL}	Parasitic power losses (W)
p_t^{Gross}	Gross power in the CSP plant (W)
p_t^{Net}	Net power from the CSP plant (W)
t	Index set for hours

reliability. The considered strategies are as follows:

1. To maximize the hours of power delivered at the minimum power output of the CSP after sunset;
2. To maximize the power delivered at the maximum power output of the CSP after sunset; and
3. A variable profile based on the hourly demand.

The final strategy consists of a variable discharge profile that allows the CSP plants to adapt their power delivery schemes to the demand. In periods of high/low demand, the CSP plants increase/decrease their power output, if possible. The discharge strategies should be obtained using an optimization method that maximizes the reliability of the power system. A similar approach was presented in Ref. [20], where the optimal use of a CSP plant with storage was assessed to maximize the unit profitability. Obtaining the optimal solution of the discharge strategies implies the incorporation of the optimization problem into the SMC method. Therefore, the required computational time could be very high. The solution applied to the variable strategy is to avoid the optimization and use demand time series for each year to program the variable discharge profile.

5.4. Wind power

The modelling of wind technology is based on the historical hourly power time series covering the period of 2007–2017. These data are also available from the Spanish TSO [22]. New power time series are created using the aforementioned MBB technique. The conditions necessary to correctly apply the MBB method are met.

The modelling of all renewable technologies has been described, and Fig. 6 represents an average week in winter and summer in a random year. The figure is an example of the time series that have been built with the models described and are used as data inputs in the SMC simulations.

6. Results

The simulations that have been performed consider the Spanish power system characterized in the previous section. In this system, multiple aggregations of PV, CSP and wind have been introduced from 1 GW to 14 GW in steps of 1 GW. These aggregations reflect a power penetration level from 2% to 25%, and the penetration level can be formulated as follows:

$$\text{Penetration} = \frac{\sum \text{Renewable}^{\text{capacity}}}{\sum (\text{Renewable}^{\text{capacity}} + \text{Conventional}^{\text{capacity}})} x100\% \quad (11)$$

where $Renewable^{capacity}$ is the total rated renewable power aggregated in the system in MW and $Conventional^{capacity}$ is the total rated coal, gas and nuclear power installed in MW.

All the reliability simulations were assessed with values of

Table 3
Capacity and reliability characteristics of power units.

Capacity Characteristics						Reliability Characteristics		
Nº Units	Nominal Power (MW)	Total Power (MW)	Mean Power (MW)	Max Power (MW)	Min Power (MW)	FOR[a] (%)	MTTF[b] (hours)	MTTR[c] (hours)
Coal units								
5	(400–599)	2783	557	570	536	5.35	604.26	34.16
18	(300–399)	6191	344	355	300	5.63	512.04	30.55
4	(200–299)	1006	251	296	206	8.99	472.91	46.71
3	(100–199)	436	145	154	138	5.57	188.26	11.10
1	(1–99)	52	52	52	52	9.40	182.73	18.96
Combined cycle units								
51	(200–900)	24948	489	859	275	4.71	1881	92
Nuclear (Boiling water reactor) unit								
1	(1000+)	1064	1064	1064	1064	1.49	3469	52
Nuclear (Pressurized water reactor) units								
5	(1000+)	4066	1016	1045	1003	3.32	3852	132
2	(900–999)	1988	994	996	992	3.95	4429	182
CSP units								
8	(1000–14000)	Depending on the aggregate penetration[d]	1.94	2941	58.24			

[a] Forced Outage Rate.
[b] Mean Time To Failure.
[c] Mean Time To Repair.
[d] The installed power CSP depends on the aggregate penetration in the system and is distributed equally among the installed units.

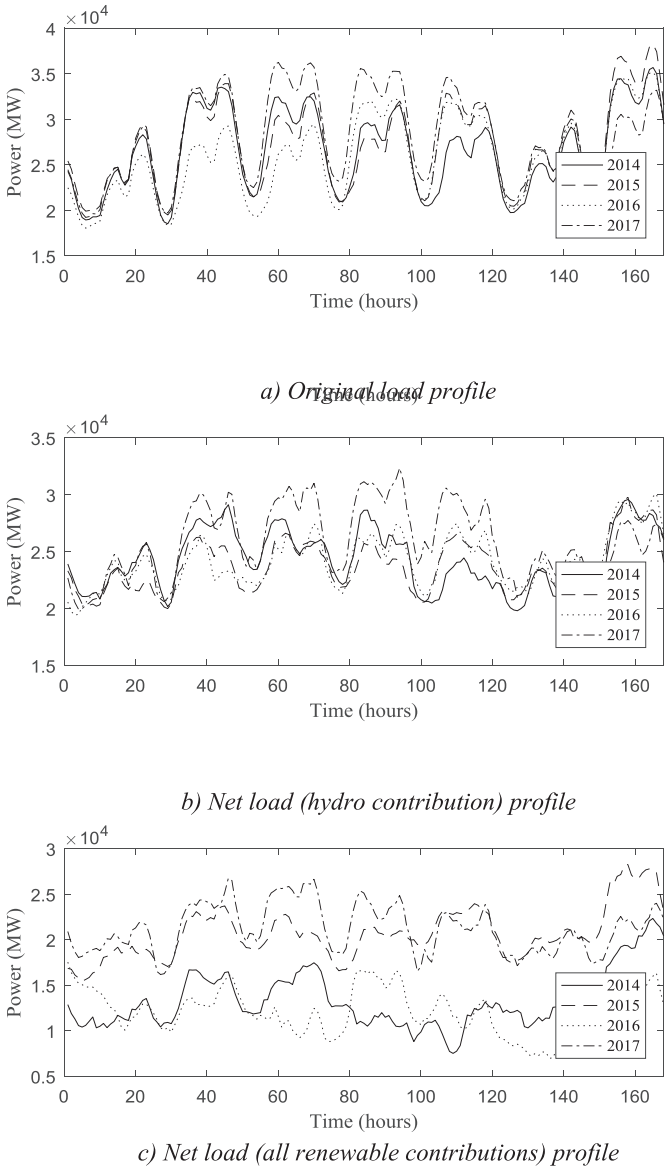

a) Original load profile

b) Net load (hydro contribution) profile

c) Net load (all renewable contributions) profile

Fig. 5. Original load and net load of the Spanish electrical power system.

$\beta_{max} = 0.03$ and $y_{max} = 6000$ years. Both parameters define the stopping criteria for SMC simulations (Fig. 2). The assessment considers three Spanish power system scenarios to reproduce the state of the current Spanish power system.

- Scenario 1. The load is represented by the original demand profile shown in Fig. 5(a).
- Scenario 2. The load is represented by the net load profile after removing the hydro contribution from the original demand profile (Scenario 1). This load profile is shown in Fig. 5(b). Hydro penetration represents 13% in terms of total energy.
- Scenario 3. The load is represented by the net load profile after wind, hydro and solar contributions are removed from the original demand profile (Scenario 1). This load profile is shown Fig. 5(c). The energy contributions of these technologies to the total load are 4.8%, 25% and 2.5% for PV, wind and CSP, respectively.

For comparison, the generation and demand in all scenarios are

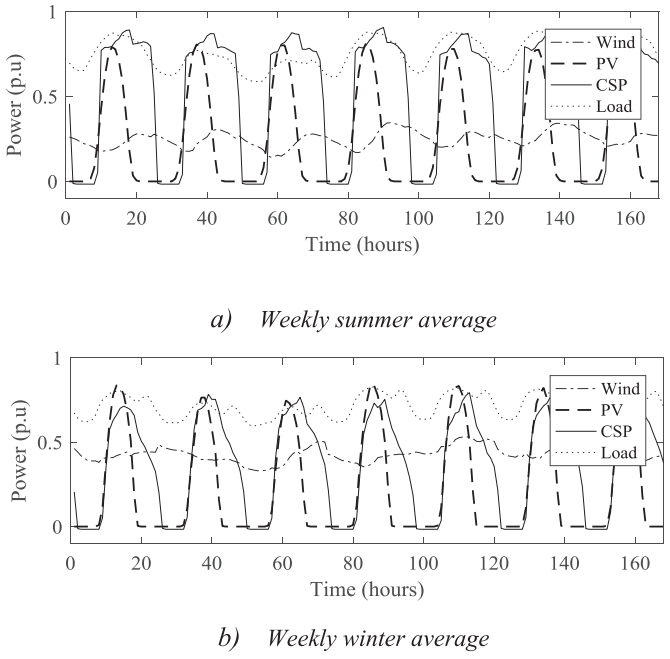

a) Weekly summer average

b) Weekly winter average

Fig. 6. Average power curve shapes for a random year used in the SMC simulations.

levelled to obtain the reliability level of the PSB (Fig. 3) at the same level. These levels are a target level fixed at 2.4 h per year. Although this reliability level is lower than those of real systems, it can be used as a reference for comparison. This target level is often used in adequacy studies, such as in Refs. [2,6,30,31]. The target is reached by modifying the average annual value of the load power time series.

6.1. Capacity credit results and EFC methodology

The obtained values of EFC are presented in Fig. 7. All the evaluated technologies are included in the system as the aggregated capacity. The installed capacity is represented by a penetration interval of 2–25% in terms of the total power (see Eq. (11)). Moreover, the three scenarios proposed are applied to all technologies.

The EFC values have similar trends for PV and CSP technologies. Both technologies yield better results in scenario 2 compared to the results for the other two scenarios. Conversely, scenario 3 provides the worst CC results for PV and CSP. The results indicate that hydropower helps in the aggregation of new solar power from the reliability perspective.

Regarding wind technology, the EFC values are practically the same for all scenarios. As the integration of wind power in the system increases, the CC decreases more slowly than in the solar case. At low penetration levels, sun-dependent technologies have higher CCs. In contrast, at a high penetration level, the CC of solar is smaller than or equal to the CC of wind. The differences among results can be explained in part by the way that each technology delivers power. CSP and PV units deliver power close to their capacity only a few hours per day. However, wind technology delivers less power, although it is distributed throughout the day. It should be noted that CSP units, which have a given storage capacity, improve the CC results at low penetration levels because the storage extends the hours of power delivery.

In accordance with the differences in the CC results for the proposed scenarios, previous studies, for instance Refs. [7,17], have demonstrated that the correlation between the demand and

generation has an important effect on the CC results. In fact, the original load profile is correlated with solar technologies because PV and CSP deliver maximum power at the same hour as the peak load. Thus, the greater the installed capacity of renewable power in the system is, the greater the deformation of the original load. Therefore, a lower correlation between the demand and renewable generation affects the CC of solar technologies but not the wind CC. In contrast, according to Fig. 5(b), hydropower maintains the original shape of the demand curve by smoothing extreme values with load shifting and valley filling strategies. These effects reduce the power demand at times when solar technologies are not available, resulting in better CC results for solar.

6.2. Comparison with the capacity value and NREL methodology

The NREL provides CV results for PV, wind and CSP technologies in the WWSIS study [6]. This study, which analysed the reliability contributions of renewables, was conducted in the western region of the United States, and the results differ considerably from those shown in Fig. 7 because the methodology used is different. Therefore, to compare the CV approaches, the NREL methodology, which is defined in Ref. [7], is described below and is applied to the Spanish power system presented.

First, it is important to note that the CV of the NREL methodology is based on the fraction of the capacity that is available during periods of high net demand:

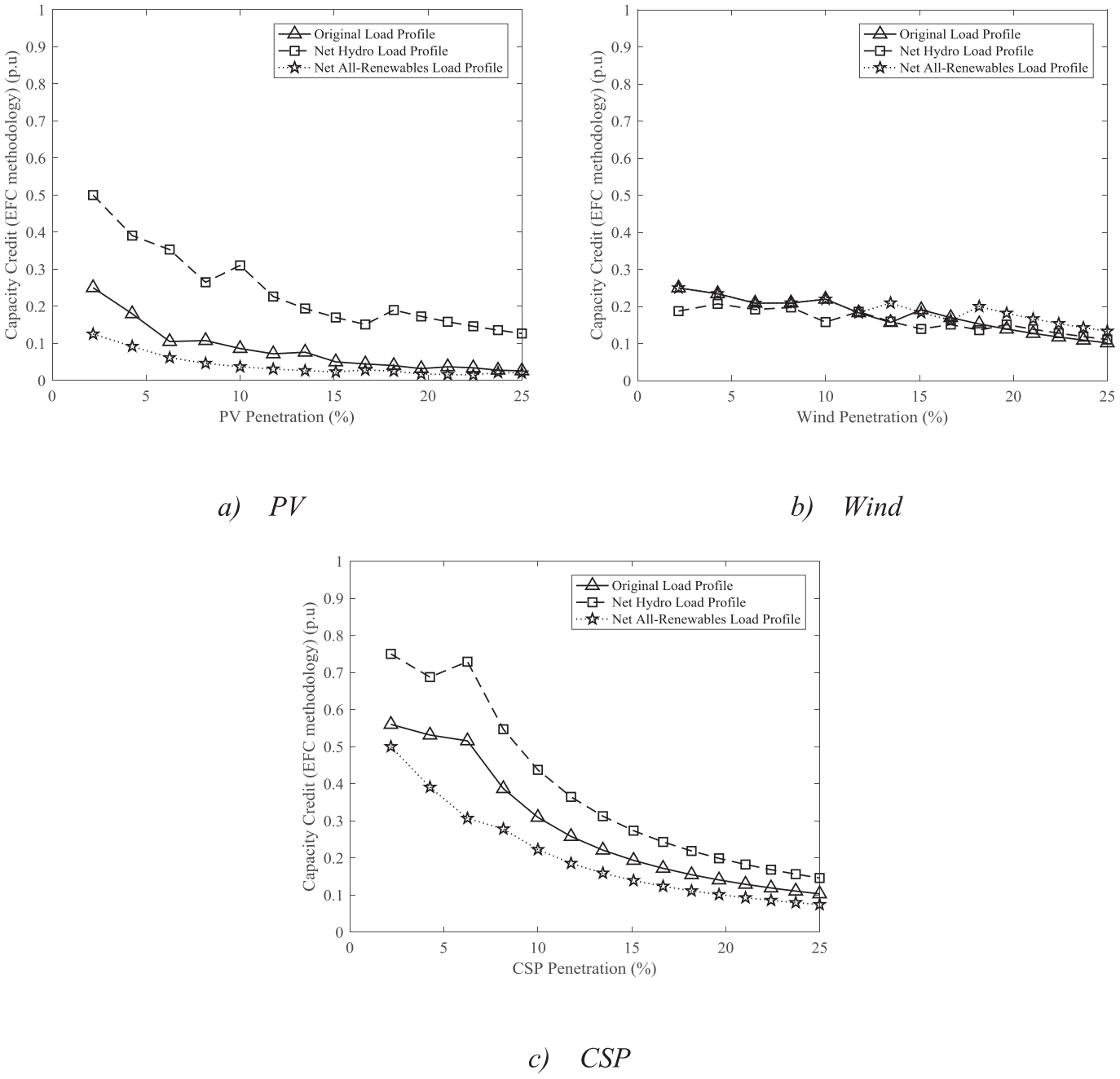

Fig. 7. CCs of PV, wind and CSP based on the EFC methodology.

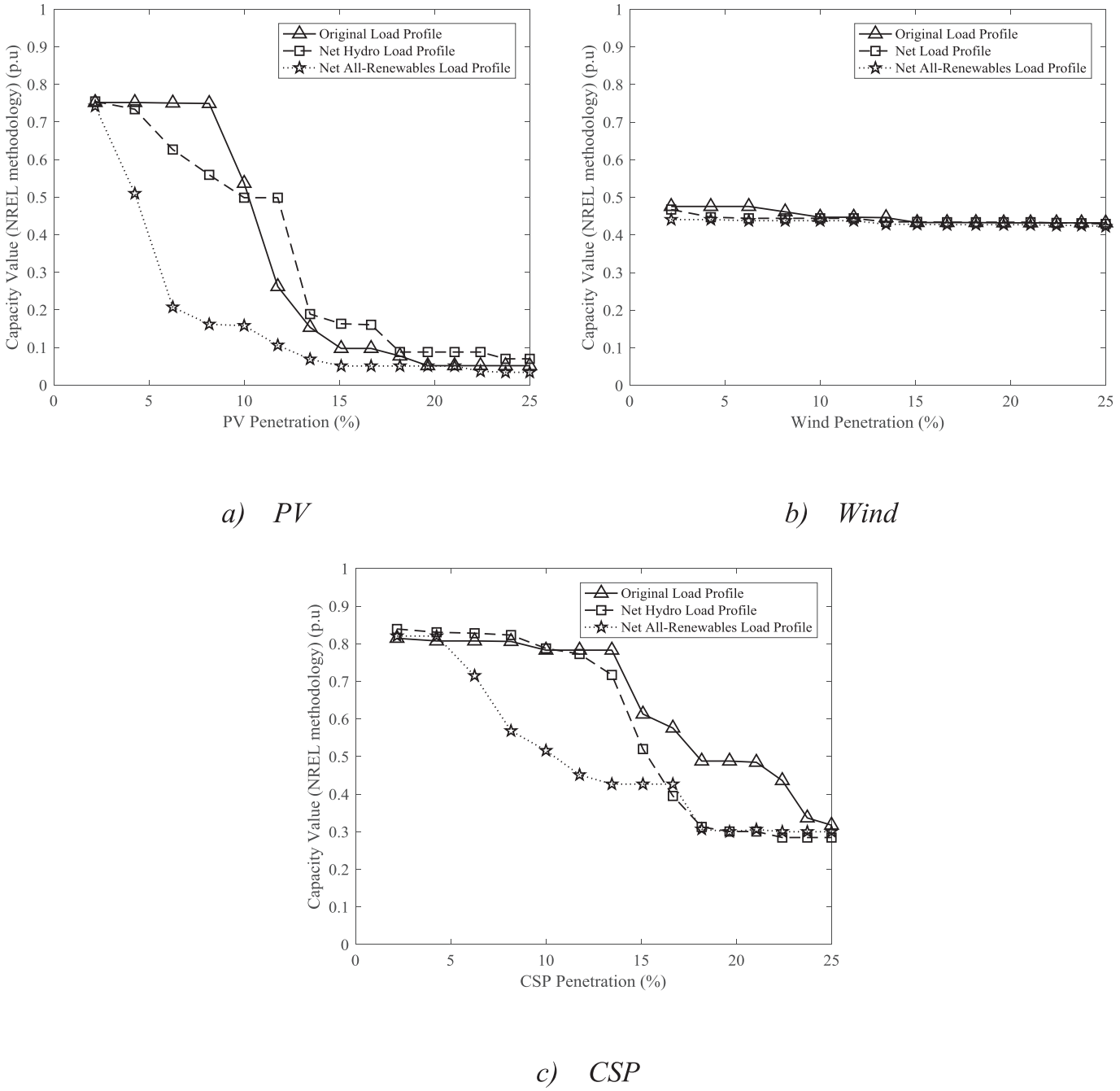

Fig. 8. CVs of PV, wind and CSP based on the NREL methodology.

$$\text{Capacity Value} = \frac{NG_t^{power}}{NG^{capacity}}, \forall t : t \in T^{\text{High Demand}} \quad (12)$$

where NG_t^{power} is the power delivered by the new generation power plant added to the system in hour t, NG_t^{capacity} is the rated power of new generation and $T^{\text{High Demand}}$ is the set of hours of high demand.

The results obtained based on the NREL methodology applied to the Spanish power system are presented in Fig. 8. With this methodology, the results are different from those obtained previously with the EFC method. For the wind case, the CV remains constant between 0.42 and 0.47 for all penetration ranges. These values differ from the values provided by the NREL in the WWSIS report, with CV values of 0.12 and 0.11 for penetration values of 10% and 20%, respectively. In the case of Spain, there is a difference of approximately 0.3 between the CV and CC values.

The CV for solar technology displays similar results. Based on the data in Fig. 8, two clearly differentiated zones can be seen. One zone has high CVs for PV and CSP at low penetration levels, and the other zone has low CVs at high penetration levels. One reason for this behaviour is the “duck chart” effect that occurs in the net load curve after solar aggregation. This effect is explained in Ref. [32], and it can be seen in this study in Fig. 9 and Fig. 10 for PV and CSP, respectively. At low penetration levels, peaks in the net demand are in the middle of the day. When the solar penetration increases to approximately 13% for CSP and 7% for PV, the peak net load shifts to

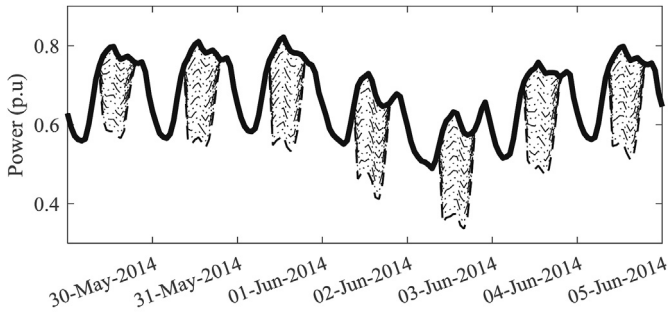

a) Original load profile scenario: weekly

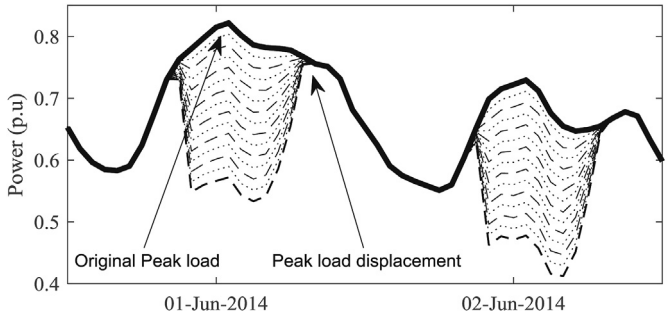

b) Original load profile scenario: daily

Fig. 9. Net load for all PV contributions.

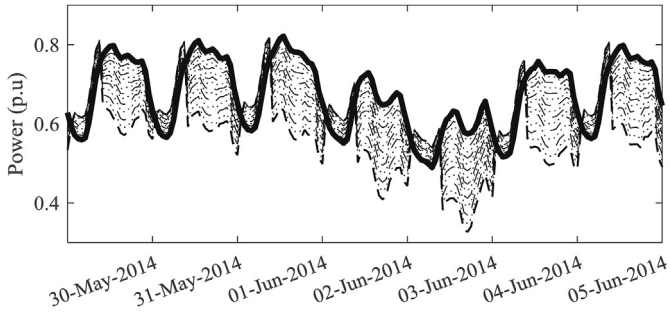

a) Original load profile scenario: weekly

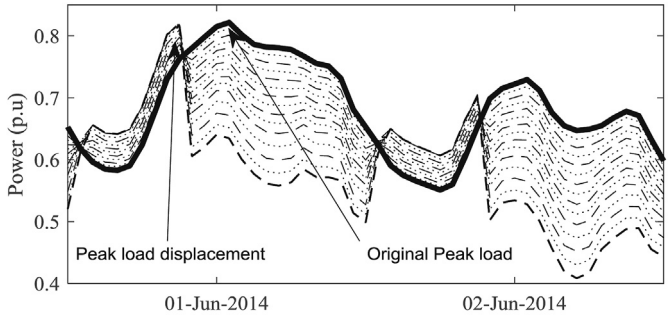

b) Original load profile scenario: daily

Fig. 10. Net load for all CSP contributions.

the final hours of the day. Due to this peak displacement of the net load, the set of hours $T^{HighDemand}$ from Eq. (12) changes drastically. In this new set of hours, the power delivery by solar technologies is not close to the rated capacity, which implies a CV reduction. CSP units yield better results than PV because they can increase the power delivered in hours of low solar radiation due to their storage capability.

The CV values obtained in this study and the WWSIS report for CSP units are similar. However, for PV, the difference reaches 0.35. This difference is not significant because the range of penetration evaluated in the WWSIS study is small.

6.3. Storage strategy results

The CC results in Fig. 11 vary depending on the storage strategy.

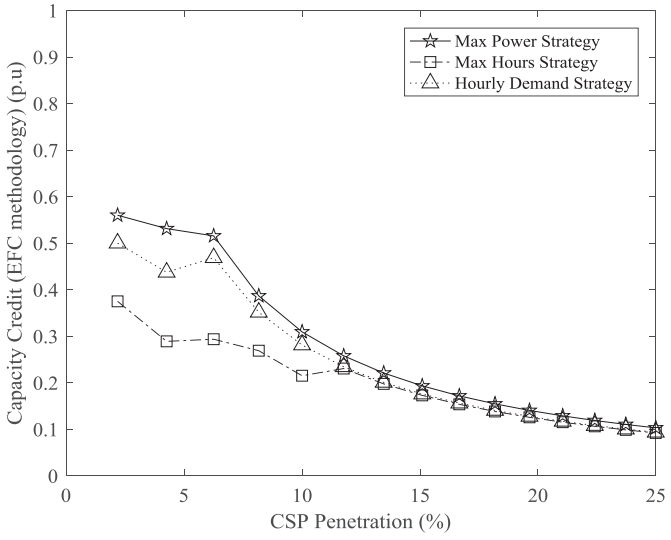

a) EFC methodology

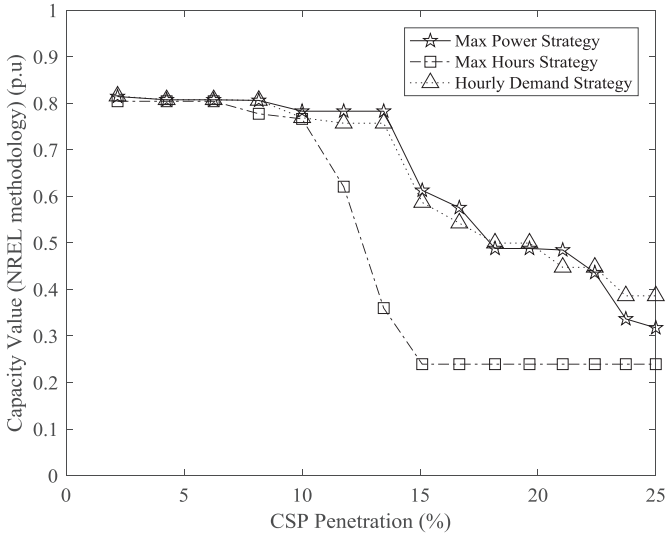

b) NREL Methodology

Fig. 11. CC and CV for the different storage strategies proposed for CSP units.

Table 4
ENTSO-e future scenarios for the Spanish power system.

		Power system configuration. Installed Capacity (GW)						
		Coal power	Combined cycle	Nuclear	Hydro	Wind	PV	CSP
Scenarios	Best Estimate 2025	4.6	24.5	7.1	21.8	28.9	19.9	2.3
	Distributed generation 2030	0.8	24.5	7.1	23	31	47.1	2.3
	European Commission 2030	3.8	27.9	7.4	23	34.5	25.8	6.1
	Sustainable Transition 2030	4.6	24.5	7.1	23	31	40	2.3

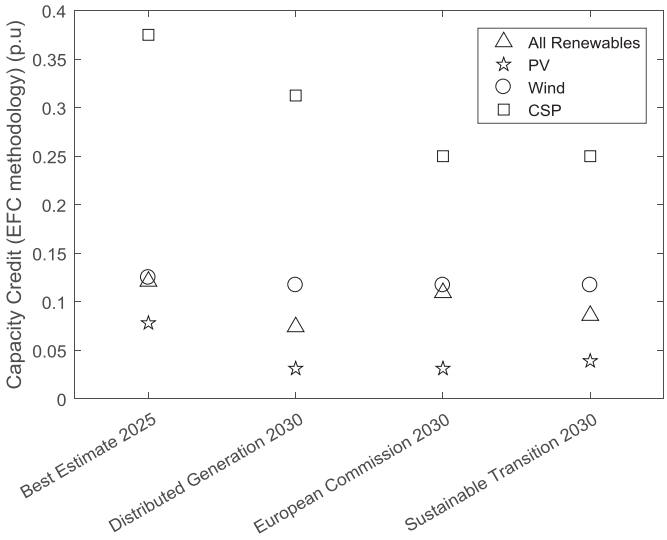

Fig. 12. CC for ENTSO-e scenarios.

These results are obtained when scenario 1 is considered. For the EFC results, the CC obtained differs at low penetration levels. In contrast, the NREL methodology displays differences that are more appreciable at high penetration levels. The differences occur because varying the storage strategy affects the amount of delivered power in high demand periods. Therefore, the CV may increase according to Eq. (12).

6.4. Future Spanish power system

In this subsection, the EFC method is applied for future configurations of the Spanish system proposed by the ENTSO-e in the most recent version of the mid-term adequacy forecast (MAF). These configurations are presented in Table 4. The EFC analysis is applied for all renewables together and for each renewable technology separately. The results are shown in Fig. 12.

The best-estimate scenario for 2025 is the scenario that yields the best CC results for renewables in combination and separately. Overall, the CC results are very low due to the high penetration of renewables in all scenarios. The penetration of wind and solar in all scenarios is 46.83% in the best-estimate scenario, 59.20% in the distributed generation scenario, 43.89% in the European Commission scenario and 55.32% in the sustainable transition scenario. In addition, it is important to note that CSP technology yields the best reliability contribution for all renewables, and the contribution is higher than the set of all renewables together because the power penetration level is low. The contribution of PV technology to the reliability of all scenarios is negligible.

To show the correlation between the power output from all renewable technologies and the load, Fig. 6 shows the weekly average power curves. Furthermore, the results illustrate how storage in CSP plants affects the corresponding contribution to reliability because high-energy production is maintained after sunset.

7. Conclusions

A reliability analysis of the most important renewable technologies was developed to assess the reliability contributions of PV, CSP and wind technologies in the Spanish power system. The following conclusions were obtained from the study.

1) The methodologies used to calculate the CC and CV values yielded different results that cannot be directly compared. Although both methodologies reflected high contributions with low renewable penetration and low contributions with high renewable penetration, the EFC methodology is more precise because it considers each hour of the year, and the methodology used by the NREL only considers high demand hours.
2) Based on the differences among the three proposed scenarios, the CC results for EFC indicate that hydropower contributes to the integration of solar power into the system. Moreover, when renewable penetration increases, the contribution to reliability decreases. The issue arises because the renewable contribution to energy production influences the net load and reduces the correlation between the demand and renewable production, which in turn implies a reduction in the contribution to reliability for newly aggregated renewable power.
3) The storage strategies proposed in CSP units affect the reliability, although this effect is minimal. Storage strategies are proposed as examples to illustrate how these strategies affect reliability, and they are not optimal due to computational limitations. Further studies should be proposed with simplifications to avoid constructing a complex problem involving optimization together and SMC simulations, which may be unsolvable.
4) The future power systems proposed by the ENTSO-e include high shares of solar and wind and low use of fossil fuel units. Although these renewables make a notable contribution to energy production, their contribution to reliability is low. Therefore, an important role of conventional generation is to meet the reliability target.

Acknowledgments

This work was supported by the University Carlos III of Madrid under project Feasibility of power systems with renewables (2009/00416/002).

References

[1] Red Eléctrica Española, El Sistema Eléctrico Español - Avance 2017, 2017, p. 36. http://www.ree.es/sites/default/files/downloadable/avance_informe_sistema_electrico_2017_v3.pdf. (Accessed 17 May 2018).
[2] R. Billinton, R.N. Allan, Reliability Evaluation of Power Systems, second ed., Plenum Press, New York, 1996.
[3] R. Billinton, W. Li, Reliability Assessment of Electric Power Systems Using Monte Carlo Methods, Plenum Press, New York, 1994.
[4] M. Matos, J.P. Lopes, M. Rosa, R. Ferreira, A. Leite da Silva, W. Sales, L. Resende,

L. Manso, P. Cabral, M. Ferreira, N. Martins, C. Artaiz, F. Soto, R. López, Probabilistic evaluation of reserve requirements of generating systems with renewable power sources: the Portuguese and Spanish cases, Int. J. Electr. Power Energy Syst. 31 (2009) 562–569, https://doi.org/10.1016/j.ijepes.2009.03.031.
[5] R. Title, R. Date, 2016 Long-Term Reliability Assessment, 2016. https://www.nerc.com/pa/RAPA/ra/ReliabilityAssessments DL/2016 Long-Term ReliabilityAssessment.pdf. (Accessed 15 March 2019).
[6] G. Energy, Western Wind and Solar Integration Study, Executive Summary, New York, 2010, p. 40, https://doi.org/10.2172/1037937.
[7] P. Denholm, M. Hummon, Simulating the Value of Concentrating Solar Power with Thermal Energy Storage in a Production Cost Model, 2012. https://www.nrel.gov/docs/fy13osti/56731.pdf.
[8] ENTSO-E, Mid-term Adequacy Forecast 2017, 2017. https://docstore.entsoe.eu/Documents/SDCdocuments/MAF/MAF_2017_report_for_consultation.pdf. (Accessed 15 March 2019).
[9] North American Electric Reliability Corporation, Reliability Assessment Guidebook, 2012, p. 81. https://www.nerc.com/comm/PC/Pages/Reliability AssessmentSubcommittee (RAS)/Reliability-Assessment-Guidebook.aspx. (Accessed 20 February 2019).
[10] M. Milligan, Methods to Model and Calculate Capacity Contributions of Variable Generation for Resource Adequacy Planning, 2011. IVGTF1-2, https://www.nrel.gov/docs/fy11osti/51485.pdf. (Accessed 18 March 2019).
[11] A. Keane, M. Milligan, C.J. Dent, B. Hasche, C. D'Annunzio, K. Dragoon, H. Holttinen, N. Samaan, L. Soder, M. O'Malley, Capacity value of wind power, IEEE Trans. Power Syst. 26 (2011) 564–572, https://doi.org/10.1109/TPWRS.2010.2062543.
[12] M. Amelin, Comparison of capacity credit calculation methods for conventional power plants and wind power, IEEE Trans. Power Syst. 24 (2009) 685–691, https://doi.org/10.1109/TPWRS.2009.2016493.
[13] S.H. Madaeni, R. Sioshansi, P. Denholm, The capacity value of solar generation in the Western United States, IEEE Power Energy Soc. Gen. Meet. (2012) 1–8, https://doi.org/10.1109/PESGM.2012.6345521.
[14] S.H. Madaeni, R. Sioshansi, P. Denholm, Estimating the capacity value of concentrating solar power plants with thermal energy storage: a case study of the southwestern United States, IEEE Trans. Power Syst. 28 (2013) 1205–1215, https://doi.org/10.1109/TPWRS.2012.2207410.
[15] T. Gafurov, M. Prodanovic, J. Usaola, Modelling of concentrating solar power plant for power system reliability studies, IET Renew. Power Gener. 9 (2015) 120–130, https://doi.org/10.1049/iet-rpg.2013.0377.
[16] C. Grigg, P. Wong, The IEEE reliability test system -1996 a report prepared by the reliability test system task force of the application of probability methods subcommittee, IEEE Trans. Power Syst. 14 (1999) 1010–1020, https://doi.org/10.1109/59.780914.
[17] M. Ding, Z. Xu, M. Ding, Z. Xu, Empirical model for capacity credit evaluation of utility-scale PV plant, IEEE Trans. Sustain. Energy 8 (2017) 94–103, https://doi.org/10.1109/TSTE.2016.2584119.
[18] D. Santos-Martin, S. Lemon, SoL – a PV generation model for grid integration analysis in distribution networks, Sol. Energy 120 (2015) 549–564, https://doi.org/10.1016/j.solener.2015.07.052.
[19] System Advisor Model (SAM). https://sam.nrel.gov, 2016.
[20] R. Dominguez, L. Baringo, A.J. Conejo, Optimal offering strategy for a concentrating solar power plant, Appl. Energy 98 (2012) 316–325, https://doi.org/10.1016/j.apenergy.2012.03.043.
[21] M. de A.G. España, Sistema de información agroclimática para el regadío, 2017. http://eportal.mapama.gob.es/websiar/Inicio.aspx. (Accessed 5 June 2017).
[22] Red Eléctrica España (REE), ESIOS, 2017. https://www.esios.ree.es/es. (Accessed 26 August 2017).
[23] P. Chen, T. Pedersen, B. Bak-Jensen, Z. Chen, ARIMA-based time series model of stochastic wind power generation, IEEE Trans. Power Syst. 25 (2010) 667–676, https://doi.org/10.1109/TPWRS.2009.2033277.
[24] A. Sturt, G. Strbac, Times-series modelling for the aggregate Great Britain wind output circa 2030, IET Renew. Power Gener. 7 (2013) 36–44, https://doi.org/10.1049/iet-rpg.2012.0040.
[25] J. Usaola, Synthesis of hourly wind power series using the Moving Block Bootstrap method, in: 2014 Int. Conf. Probabilistic Methods Appl. to Power Syst, IEEE, 2014, pp. 1–6, https://doi.org/10.1109/PMAPS.2014.6960602.
[26] North American Electric Reliability Corporation (NERC), Generating Unit Statistical Brochures, 2017. https://www.nerc.com/pa/RAPA/gads/Pages/Reports.aspx. (Accessed 18 March 2019).
[27] J. Juan, I. Ortega, Reliability analysis for hydrothermal generating systems including the effect of maintenance scheduling, IEEE Trans. Power Syst. 12 (1997) 1561–1568, https://doi.org/10.1109/59.627859.
[28] C. González, J. Juan, C. Gonza, Reliability evaluation for hydrothermal generating systems: application to the Spanish case, Reliab. Eng. Syst. Saf. 64 (1999) 89–97, https://doi.org/10.1016/S0951-8320(98)00055-6.
[29] P. Tapetado, J. Usaola, Comparison of different photovoltaic models in a capacity credit evaluation, in: 7 Sol. Integr. Work, 2017.
[30] E. Lannoye, D. Flynn, M. O'Malley, Evaluation of power system flexibility, IEEE Trans. Power Syst. 27 (2012) 922–931, https://doi.org/10.1109/TPWRS.2011.2177280.
[31] C.K. Simoglou, E.A. Bakirtzis, P.N. Biskas, A.G. Bakirtzis, Probabilistic evaluation of the long-term power system resource adequacy: the Greek case, Energy Policy 117 (2018) 295–306, https://doi.org/10.1016/j.enpol.2018.02.047.
[32] P. Denholm, M. O'Connell, G. Brinkman, J. Jorgenson, Overgeneration from solar energy in California, in: A Field Guide to the Duck Chart, 2015, https://doi.org/10.2172/1226167.